EUROPEAN COOPERATION
IN THE FIELD OF SCIENTIFIC
AND TECHNICAL RESEARCH

EURO-COST

COST 2100 TD(10)11048
Aalborg, Denmark
June 2-4, 2010

SOURCE: - University of Bristol
- TREL, Toshiba Research Europe Limited
United Kingdom

Improved Antenna Mounting Method for UWB BAN Channel Measurements

William Thompson[1], Rafael Cepeda[2], Simon Armour[1], Mark A. Beach[1]
[1] University of Bristol
Department of Electrical and Electronic Engineering
Merchant Venturers Building, Woodland Road
Bristol, BS8 1UB
UNITED KINGDOM
[2] Toshiba TRL
32 Queen Square
Bristol, BS1 4ND
UNITED KINGDOM
Phone: (1) + 44 (0) 117 331 5052
Fax: (2) + 44 (0) 117 906 0701
Email: {W.Thompson, Simon.Armour, M.A.Beach}@bristol.ac.uk
Rafael.Cepeda@toshiba-trel.com

Improved Antenna Mounting Method for UWB BAN Channel Measurements

William Thompson[1], Rafael Cepeda[2], Mark A. Beach[1], Simon Armour[1]

May 26, 2010

[1] University of Bristol, Department of Electrical and Electronic Engineering, Merchant Venturers Building, Woodland Road, Bristol, BS8 1UB, UNITED KINGDOM
[2] Toshiba TRL, 32 Queen Square, Bristol, BS1 4ND, UNITED KINGDOM

Abstract

In this paper, a mounting method is proposed for antennas used in ultra wideband (UWB) body area network (BAN) channel sounding, which reduces the antenna's electromagnetic coupling to the human body. Coupling with the body is shown to distort the free space characteristics of the antenna. An antenna mount modification is proposed to reduce this distortion, and decrease the variation in antenna characteristics when mounted. The antennas reflection coefficient from 4 to 9 GHz is used to assess the coupling of two UWB BAN antennas when they are mounted at different distances from the skin and at several locations on the body. The free space characteristics of the modified antennas are also tested, showing a reduction of up to 4.7 dB of radiated power into the body. The modified antennas are tested in BAN measurement campaigns showing the fading depth and coherency time of the channels.

1 Introduction

The popularity of portable media and monitoring devices has resulted in wireless communications systems increasingly moving from fixed location transmitters and receivers, to mobile ones, and even both the transmitter and receiver being carried by a single user, forming a body area network (BAN) [1, 2]. A limiting factor in many high data rate BAN applications is the battery life, resulting in a need for energy efficient systems, ultra wideband (UWB), operating between 3.1 to 10.6 GHz, is seen as a technology that can meet this growing demand for high data rate transmissions at very low power levels [3].

Considerations for the propagation channel are an important part in the design of communication systems. Hence significant effort has been undertaken to characterise UWB local area network (LAN) channels, resulting in standardised models for several environments [4]. However, UWB BAN channel characterisation is far less advanced, which is in part due to the great number of variables in the BAN environment, such as the body and posture of the user, antennas and mounting methods [5].

When an antenna is placed near a subject's body in BAN measurements, the antenna often electromagnetically couples with the body and this causes the antennas characteristics to alter, how much depends on the type of antenna, distance from the body surface and the permittivity of the surrounding tissue [6, 7]. These variations in antenna characteristics can cause significant problems when measuring moving BAN channels, since the movement of the subject can cause fluctuations in antenna characteristics as well as the channel. Research in [2] suggests the use of magnetic antennas to minimise the coupling of the antennas to the body. However, for UWB, the choice of suitable antennas can be small, so a method that decreases the coupling between any UWB antenna and the body can be very desirable.

Although real devices are affected by antenna coupling, for channel modelling the emphasis is on characterising the channel, while also being aware of the effects of the antenna. However, if the antenna characteristics are varying, it then becomes very complex to distinguish between changes due to the antenna or the channel.

Ideally, for channel sounding, the antenna characteristics would not alter when the antenna is in free-space or mounted onto a body, as this would result in the free-space characterisation of the antenna still being valid when the antenna is mounted; however, in practice, antennas normally couple with items placed within their near-field [8]. To solve this problem, modifications were made to two UWB antennas, one commercially available antenna [9] and one fabric antenna [10], both suitable for BAN channel sounding, to limit their coupling with the body during BAN measurements. The effects of body coupling on return loss were studied, as well as far-field radiation pattern analysis of the modified antennas when they were off the body. The work shows that a simple modification can significantly reduce the body coupling of the antenna, allowing more accurate characterisation of the antenna when it is in free-space. The modification also made the antenna less sensitive to the mounting location on the body.

To study the effects of placing the antennas on the body, the reflection (S_{11}) and transmission (S_{21}) coefficients of the antennas were measured using a vector network analyser (VNA), from 4 to 9 GHz, as the antennas were slowly moved away from the body. To test any variability due to the mounting location of the antenna on the body, the reflection coefficient tests were repeated at four locations; the sternum, top of the thigh, the middle of the abdomen and the top of the arm.

[11–13] showed that most of the transmitted energy at UWB frequencies is absorbed into the body, and does not pass through it. This causes the effective efficiency of the antenna to decrease, since the energy radiating into the body is lost. The proposed antenna modification uses this property of UWB signals by employing radar absorbent material (RAM) to shield the antenna from the user. This reduces the radiation into the body, but still allows the principal propagation mechanisms of UWB BAN.

To test the modifications in a measurement environment, a UWB periodic correlation based channel sounder [14, 15] was used to take moving BAN channel measurements in an office environment. Subsequently, the coherency time and fading depth of the channels were estimated from the measurement data.

2 Equipment

The first antenna under test (AUT) was a commercially available SkyCross SMT-3TO10M-A [9], with stated operating range of 3.1 to 10 GHz, however the effective operating range of the antenna was found to be between 3.7 and 9 GHz. This antenna was chosen due to its common use in UWB BAN channel measurement campaigns [11, 13, 16–18]. The SkyCross was mounted on a printed circuit board (PCB). The total size of the antenna, PCB and SubMiniature version A (SMA) connector was 35.1x18.5x3.88 mm. Both sides of the antenna are shown in Figure 1a.

The second AUT was a fabric UWB annular slot antenna [10]. This antenna was chosen as its fabric construction allows direct integration into clothing. The operating range of this antenna was found to be between 4 and 10 GHz. The construction of the antenna was slightly modified from the design in [10] by placing all the metal of the antenna on one side of the fabric, and changing the feeding of the antenna, so that a 12 cm semi-rigid feedline was attached to an SMA connector. This removed the SMA connector from the base of the antenna, and improved its performance. As changes in the field pattern when the antenna flexed were unwanted, a 0.5 mm thick plastic sheet was attached to the antenna making it rigid. The flexing effects of the antenna are an important aspect to be characterised. However, their investigation is out of the scope of this work. The metallic size of the antenna was 40.3x31.5x1.3 mm without the feedline, the antenna was used in a measurement campaign in [19], and is shown in Figure 1b.

The antennas were analysed between 4 and 9 GHz as both antennas gave their best performance over this range. To test the coupling of the antennas with the body, the reflection coefficient was investigated. This showed the amount of energy accepted into the antenna from a 50 Ω source, which is also related to the reflection efficiency of the antenna. When the antenna couples with items within its near-field, changes in the reflection coefficient are normally noticed [13, 20]. The test location on the body used in this work, were chosen as they provide a wide variation in body composition. As the sternum has only a thin layer of skin covering bone, the thigh has a thick layer of muscle, the abdomen has the most varied composition (fat, muscle and digestive organs) and the arm is significantly smaller and more curved than the other locations.

To measure the reflection coefficients, the antennas under test (AUT) were connected to an Anritsu 37397C VNA, 801 points were measured between 3 and 10 GHz, giving a frequency resolution of 10 MHz. When the antennas were connected to the VNA, no objects were placed within 0.5 m of the antennas and the front of the VNA was shielded with RAM.

The free-space far-field radiation patterns were investigated, giving insight into the radiated powers and gains of the antennas. To measure the far-field radiation patterns and total radiated power of the antennas, measurement facilities at Ilmenau University of Technology, Germany, were used. Two identical reference horn antennas, made by Q-Par [21], were used for the measurements. The results were analysed using the two antenna method [8] to remove the reference antenna and channel characteristics from the AUT measurements.

3 Reflection Coefficient

To test the antenna coupling with the body, the antennas were strapped against the sternum, abdomen, thigh, and top of the arm, with the separation between the antenna and skin being varied between 0 and 20 mm in 5 mm steps. The reflection coefficient of the antenna were measured at each location and separation distance, the 5 mm steps in separation distance were achieved by using foam spacers, the effect of placing the foam spacers on to the antenna was tested and found not to influence its perfor-

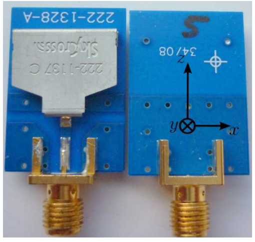

(a) SkyCross

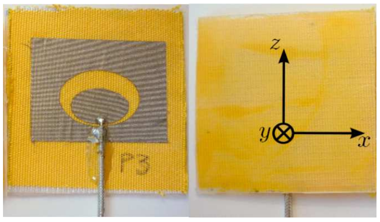

(b) Fabric

Figure 1: Tested antennas, left-hand side front, right-hand side back.

mance.

The S_{11} is related to the reflection efficiency e_r of the antenna. If it changes significantly, this affects the overall efficiency e_0 of the antenna, since

$$e_o = e_r e_c e_d,$$

where e_o is total efficiency, e_r, e_c and e_d are respectively the efficiencies due to the reflection, conductivity and dielectric. The S_{11} is related to e_r by: $e_r = (1-|S_{11}|^2)$. As it is impractical to undertake detailed characterisation of the antenna when it is mounted on the body, instead this is often undertaken in free-space. However, these results become unreliable once the antenna is placed on the body if the antenna has strong coupling with it. One method to measure the change in coupling of an antenna is to measure the variation in S_{11}.

As well as efficiency, fluctuations in the coupling also cause changes in the radiation pattern. This affects channel sounding measurements, especially if used in a moving environment, as the fluctuating antenna effects would also be embedded in the channel measurement.

To test the antennas coupling to the body, the S_{11} of the antenna was measured as it was moved away from the skin. These S_{11} results were then compared to the free-space antenna S_{11} results. Figure 2 shows both antennas S_{11} for free-space and when the antennas are mounted 5 mm away from the chest. Significant variation is noticed in the results when the antenna is mounted onto the chest such as the detuning of resonances in the antenna and increases in the reflection coefficients. For conciseness, these results are summarised in Table 1 for the antennas in free-space and when mounted on the sternum

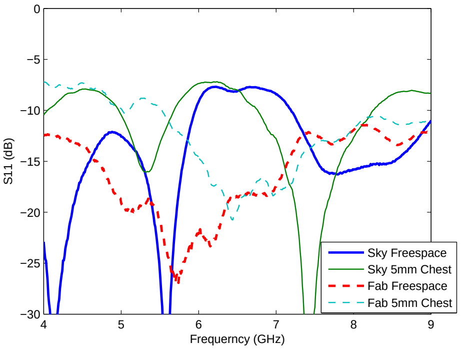

Figure 2: S_{11} results for both antennas when in free-space and when mounted 5 mm away from the chest.

Table 1: S_{11} properties of the unmodified antennas when in free-space and mounted onto the sternum (chest).

Distance from chest (mm)	SkyCross unmodified			Fabric unmodified		
	$S_{11}>$ -10dB (%)	Mean (dB)	e_r change (%)	$S_{11}>$ -10dB (%)	Mean (dB)	e_r change (%)
Free-space	24.75	-14.6	0	0	-16.32	0
0	74.25	-7.83	-18.84	33.93	-14.8	-3.83
5	40.72	-12.59	-2.71	28.94	-12.41	-4.38
10	38.72	-12.58	-2	30.74	-12.16	-4.48
15	29.94	-11.94	-3.14	24.15	-11.93	-4.09
20	67.07	-10.59	-4.55	13.97	-13.38	-2.55

(chest). The table shows the percentage of S_{11} greater than -10 dB, the average S_{11} value, and the change in reflection efficiency compared to the free-space antenna, where a positive value indicates a gain in efficiency and a negative value a loss.

For both antennas, 0 mm separation from the body results in the largest gain in percentage of S_{11} greater than -10 dB, and for the SkyCross antenna, this causes an 18% decrease in e_r. For larger separations for both antennas, the e_r decrease was around 4%, and a 2 to 3 dB increase in average S_{11} compared to the free-space antenna results. These changes were typical for all locations, with the antennas S_{11} performance significantly changing when mounted, indicating that any characterisation of the antennas in free-space would be of limited use once the antennas were mounted.

To show the amount of change in S_{11}, the magnitude of the complex correlation coefficient ($|\rho(X,Y)|$) was found between the antennas S_{11} in free-space and when mounted on the body, these results are shown in Figure 3. The correlation coefficient is given by:

$$\rho(X,Y) = \frac{E\{(X-\mu_X)(Y-\mu_Y)\}}{\sigma_X \sigma_Y} \quad (1)$$

where $E\{.\}$ is the expectation operator, X and Y are the two antennas reflection coefficient vectors with expected

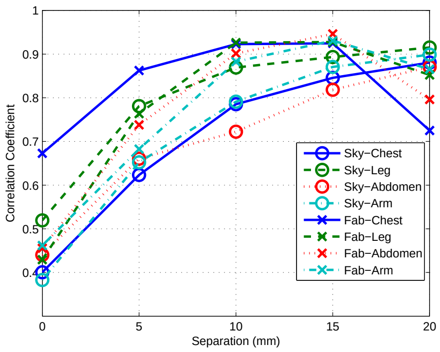

Figure 3: Correlation coefficient of antennas S_{11} when in free-space and mounted on body.

values μ_X and μ_Y, and standard deviations σ_X and σ_Y. A higher correlation coefficient between two S_{11} results shows lower coupling between the antenna and the body. Highly correlated signals provide correlation coefficients above 0.9, below 0.7 can be considered weakly correlated, and below 0.5 uncorrelated.

The results show that when the antennas are mounted directly onto the body, their response changes significantly compared to free-space, with a correlation coefficient magnitude around 0.4 to 0.5, which is considered uncorrelated. In general, as the separation increases so does the correlation, showing a decrease in coupling with increased separation. For a separation of 10 and 15 mm, the correlation of the fabric antenna could be considered high. However, the SkyCross results are lower and much more spread out compared to the Fabric antenna, making the free-space analysis of the antenna inaccurate once mounted.

To test the variation in coupling at different locations, the correlation coefficient between each location was tested and it was found that the correlation between S_{11} results for each of the separations was high regardless of where the antenna was located on the body. The largest variation was when the fabric antenna was placed directly onto the skin, when the correlation between the arm and other locations fell to 0.75. Otherwise, all other correlation coefficient results were greater than 0.88.

4 Modification

Ideally, the S_{11} would not change when the antenna is mounted onto a body, this would result in properties like the reflection efficiency remaining the same, and the antenna characteristics would not change depending on where the antenna was mounted on the body.

One possible method of achieving this is to effectively block the radiation from the back of the antenna, which should not affect the antennas overall performance once mounted on to the body, since most of the radiation at UWB frequencies is absorbed and does not radiate through the body [13].

To block the radiation from the back of the antenna a 55x55x10 mm piece of ECCOSORB AN73 RAM [22] was used to isolate the antenna from the body. Since the RAM would be fixed at a set distance, coupling with the RAM should be constant, it would also be possible to test the antenna with RAM in free-space. The RAM was placed on the skin, and measurements were taken assessing the effects of varying the separation between it and the antenna. The RAM faced the back of each antenna, which is defined as the side of the antenna facing the negative y direction in Figure 1.

As the modifications can be considered part of the antenna, the test comparing the antennas in free-space and when mounted, are between the antenna with the RAM fixed at a certain distance from the antenna when it is in free-space and mounted on the body.

Table 2 shows S_{11} properties of the antennas with the RAM when it is in free-space and mounted to the sternum. In the table, the percentage of S_{11} greater than -10 dB and average S_{11} value are shown, along with the change in reflection efficiency when the antenna and RAM is in free-space and mounted.

Comparing the results in Table 2 to the ones in Table 1, it is seen that the variation between the mounted and free-space antennas average S_{11} is below 1.2 dB for all separations for the modified antenna. This compares to an average change of over 2 dB and a maximum change of 6.7 dB for the unmodified antenna. The average change in reflection efficiency also shows low coupling of the antenna to the body, with an average change of under 0.5%, this shows a significant improvement in the stability of the reflection efficiency when the RAM is used when mounting the antenna.

To test the variation of the antennas with the RAM when in free-space and when mounted, the magnitude of the complex correlation coefficient ($|\rho(X,Y)|$) of the S_{11} was found, and the results are shown in Figure 4.

When these results are compared to Figure 3, where no RAM was used, significant improvements in the reduced coupling are noticed. For large separations of 15 to 20 mm the correlation coefficient of S_{11} falls to 0.8 for the chest and abdomen locations, this is likely due to the square piece of RAM no longer shielding the body from the direct radiation from the antenna, allowing greater coupling with the body. However, for most other separations and locations, the correlation coefficient was above 0.9, showing very strong correlation between the free-space and mounted S_{11} characteristics, with separations of 5 and 10 mm providing the best overall performance.

The correlation coefficient between the S_{11} for the dif-

Table 2: S_{11} properties of the modified antennas when in free-space and mounted onto the sternum (chest).

Distance	Modified SkyCross					Modified Fabric				
from chest	Free-space		Mounted			Free-space		Mounted		
(mm)	S_{11}>-10dB (%)	Mean (dB)	S_{11}>-10dB (%)	Mean (dB)	e_r change (%)	S_{11}>-10dB (%)	Mean (dB)	S_{11}>-10dB (%)	Mean (dB)	e_r change (%)
0	18.76	-12.9	2.99	-12.75	0.79	0	-16.58	1.8	-17.22	-0.79
5	9.78	-12.95	17.96	-13.61	0.28	0	-15.58	11.98	-15.95	-0.07
10	26.95	-12.6	31.34	-11.41	-1.01	0	-14.1	9.98	-15.79	0.42
15	36.93	-11.53	38.32	-11.02	-0.59	0	-14.64	2	-17.84	0.32
20	31.14	-11.44	34.13	-11.47	0.02	0	-17.92	0.4	-17.63	-0.28

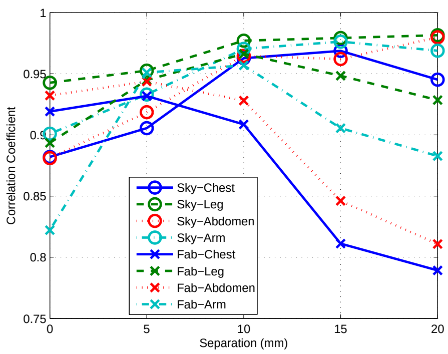

Figure 4: Correlation coefficient of modified antennas S_{11} when in free-space and mounted on body.

Table 3: Radiated Power of the antennas from the complete sphere, the positive y facing hemisphere, and negative y facing hemisphere.

	Radiation hemisphere		
	Both	Forward	Backward
SkyCross (dB)	-50.89	-54.38	-53.48
Modified SkyCross (dB)	-53	-56.08	-55.94
Difference (dB)	2.11	1.7	2.46
Fabric (dB)	-52.43	-55.52	-55.37
Modified Fabric (dB)	-55.32	-57.06	-60.14
Difference (dB)	2.89	1.54	4.77

ferent mounting locations was also calculated. The largest difference was when the fabric antenna was mounted onto the arm, with no separation between the antenna and RAM, when the correlation coefficient between this location and the other locations fell to 0.7. Otherwise, a correlation coefficient of above 0.9 was found for all locations and antennas, and for separations of 5 or 10 mm the correlation coefficient was very high at 0.97. This shows a very low sensitivity to mounting location for these antenna-RAM separations, and shows even less sensitivity than the unmodified antennas.

The transmission response of the antennas were measured in free-space to assess the effects of placing the RAM at different distances from the antenna. This was done in an anechoic chamber, with a bicone antenna [23], which operated over the full UWB bandwidth, as a transmitter, and the AUT 1 m away from it. The transmission response was measured at different RAM spacings to aid the choice of the optimum spacing for the antenna in channel sounding measurements. It was found that the variation in received power fluctuated for all the measured distances by about 2 dB. The larger separations generally gave the slightly stronger signal power. However as this was only a marginal gain, and as Figure 4 shows, the reflection coefficient changed the most when mounted onto the body for separations of greater than 15 mm. Also, for channel sounding a small antenna is desirable, as it would remain close to the user's skin. A small separation between the antenna and RAM was desirable because when the RAM was mounted directly onto the antenna, the reflection coefficient changes significantly compared to free-space, this may lead to undesired characteristics in the antenna response. A separation of 5 mm was chosen as it provides a compact antenna, with good coupling rejection and transmission power. This separation had also been used for the unmodified SkyCross antenna in [17, 18, 24] for channel sounding measurements.

To fully characterise both antennas with a RAM separation of 5 mm, the three dimensional radiation patterns were measured for each antenna. The two antenna method was used to de-embed the reference horn antenna and the channel from the measurements [8], and the antenna transfer functions were estimated, allowing the radiation intensities and the total radiated powers from the antennas to be found. The azimuth total radiation gain of both antennas is shown in Figure 5, the RAM covers both antennas azimuth angels from -180 to 0 degrees. Both antennas stronger beams are now in the positive azimuth angle directions, with the RAM suppressing radiation from the back of the antenna. The less directional behaviour of the SkyCross is also noticed in Figure 5, with the fabric antenna producing a dominant beam between 50 and 150 degrees, with deeper fades around the edges of the antenna. Since the RAM blocks significant radiation from the back hemisphere of the antennas, the difference in the radiated power from modified and unmodified antennas were found for: the complete radiation sphere, radiation from the front, and from the back hemispheres of the antennas.

Table 3 summarises the results, also showing the difference between the modified and unmodified antennas. Placing the RAM on the antennas shows a decrease in the radiation power of both the front and back hemisphere radiation for both antennas. It decreases the forward radiation by about 1.5 dB for both antennas, while the SkyCross reverse radiation decreases by 2.4 dB, and the fabric antenna by 4.7 dB. The RAM will also attenuate any reflected signal from the body, as the wave passes for a second time through the RAM.

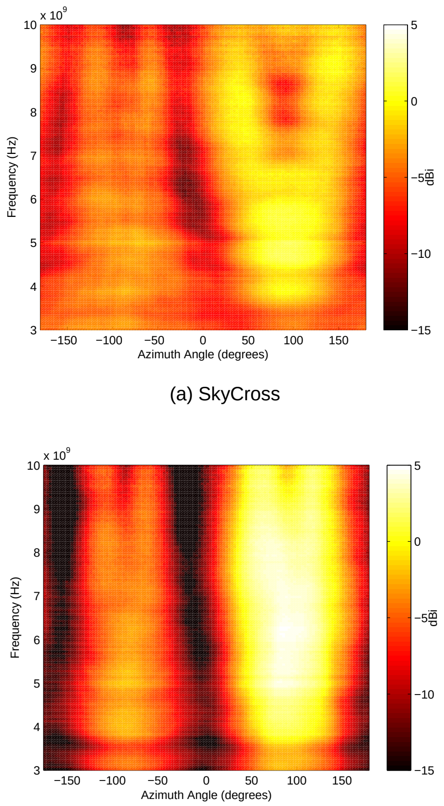

(a) SkyCross

(b) Fabric

Figure 5: Modified antenna azimuth total gain patterns for 90 degrees elevation angle.

5 Channel Sounding

To test the antennas in a channel measurement scenario, an office was used at TOSHIBA TRL, Bristol, UK, a multiple input multiple output (MIMO) UWB periodic correlation based channel sounder [14, 15, 23] was used, capable of taking measurements in moving environments, with a bandwidth and centre frequency of 6.95 GHz. The channel sounder was setup in 1x4 single input single output (SIMO) configuration, however, only a single input single output (SISO) channel was considered for this analysis.

The receive antenna was attached to the left waist, and the transmitter was mounted on the sternum (chest), right wrist, and the middle of the back between the shoulder blades, the antennas were orientated with their x axis horizontal for the sternum, back and waist locations; for the wrist location the x axis was vertical when the arm was hanging relaxed. One thousand channel impulses were measured for each transmitter location when the user stood still and walked slowly on the spot.

To find the maximum speed of movement, an identical channel sounder was tested at Ilmenau University of Technology, Germany. The test involved moving a receive antenna away from a fixed transmitter, the test was repeated several times varying the speed of motion. To find the maximum speed of motion, the time domain channel impulse response was interpolated and the phase of the peak line of sight (LOS) component was found. A maximum phase change between consecutive samples of 60 degrees was chosen. The sounder was setup so that for every outputted impulse response, it averaged 32 actual channel measurements. If the phase change was above 60 degrees, then the first and last measurement would begin to cancel, distorting the result. Therefore, consecutive outputted measurement results should have phase changes of less than 60 degrees.

The maximum movement can be found theoretically, using the sampling time of the sounder and its centre frequency (f_c). The sampling time of the sounder (T_s) using 32 hardware averages was 19.3 ms, then setting the maximum phase change ($d\theta$) to 60 degrees, the maximum

Table 4: Channel fading depths for the BAN measurements.

	Fading Depth (dB)			
	SkyCross		Fabric	
Location	Standing	Walking	Standing	Walking
Back	0.18	1.01	0.17	1.17
Chest	0.19	0.83	0.14	0.48
Wrist	0.36	3.72	0.24	3.2

speed of movement (V_{max}) is given by

$$V_{max} = \frac{(d\theta/360)C_0}{f_c T_s},$$

where C_0 is the speed of light. Giving a theoretical maximum speed of 0.37 ms^{-1}. This corresponds well with one measurement test that had an average phase change of 55 degrees, and a speed of 0.34 ms^{-1}. For all the BAN channel measurements the maximum speed of movement was kept below this speed.

In the following results, the fading depth and the coherence time of the channels for both antennas and all measurement locations are shown. The correlation coefficient R between two UWB channels at sample times t and $t+\Delta t$, with frequency response $H(f,t)$ and $H(f,t+\Delta t)$, is defined by

$$R = \frac{E\{H(f,t)H^*(f,t+\Delta t)\}}{\sqrt{E\{H(f,t)H^*(f,t)\}E\{H(f,t+\Delta t)H^*(f,t+\Delta t)\}}}$$

where the expectation is taken over frequency. The correlation time is taken as the time that R is greater than 0.75. For the tests Δt was set to multiples of the sounding time of 19.3 ms. The fading depth was found from the cumulative distribution function (CDF) of the average received power, and was defined by the fading margin between 10% and 50% of the CDF of the total received channel power.

The received power CDF for each test are shown in Figure 6, the corresponding fading depth are shown in Table 4. The stationarity of the channels when the subject is standing is shown by the very small fading depth, and almost vertical lines in the CDF plots. Due to the strong LOS components from the chest to waist, even when the user walks the fading depth is relatively small, as shown in the table. The connection between the waist and the back, does not have the strong LOS component, and so shows a larger fading depth as the user walks. The large movements of the arm cause a large fading depth when the antennas are mounted onto the wrist, as they pass from near LOS to non-LOS during each stepping motion.

The coherency time of the walking movements are shown in Figure 7, the speed of the movements results in a longer coherency time than would be expected for normal walking speed. However it does show the wrist having a much smaller coherency time than the other locations,

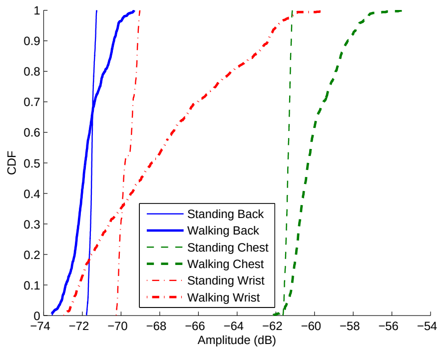

(a) SkyCross

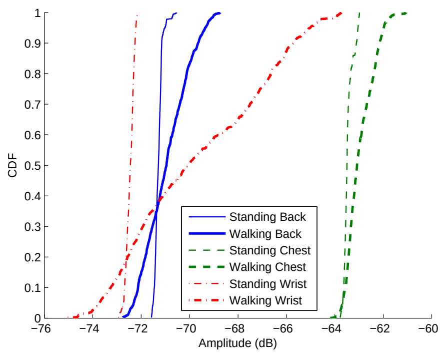

(b) Fabric

Figure 6: CFD of received channel powers of the BAN channel measurements.

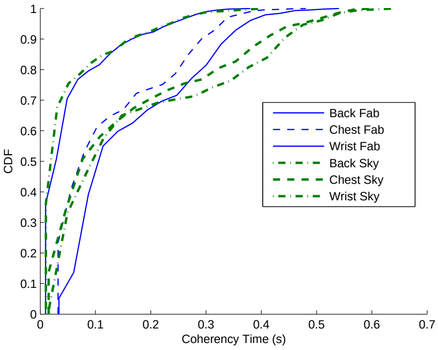

Figure 7: Coherency time of BAN channel measurement, for the user walking slowly on the spot.

this is due to the relative environment changing at a much greater speed as the arm swings during the movement.

6 Discussion

The presented antenna mounting modification provides lower antenna coupling with the body, resulting in less variation in the antenna characteristics when the antenna is mounted onto a body, allowing for more accurate off body characterisation of the antenna. Although this modification was proposed to minimise the antenna coupling for channel measurements, it could also be used in consumer products, as the modification reduces unnecessary and possibly harmful radiation into the body. It also decreases the uncertainty of antenna variation in link budget design.

The current form of the antenna module is reasonably thick, since 1 cm of RAM and 5 mm of foam spacer separates the antenna from the skin. If an alternative type of RAM was used, such as ECCOSORB FGM-U [25], similar performance could be achieved with a RAM thickness of about 2 mm. Further studies of the separation of the RAM and antenna may also lead to a reduced separation, producing a much thinner final device.

7 Conclusion

A simple ultra wideband (UWB) body area network (BAN) antenna mounting modification has been proposed that decreases the electromagnetic coupling of an antenna when mounted on to the human body. This modification involved isolating the antenna by placing radar absorbent material between it and the body. The modification was tested on two antennas, and was found to reduce the variation in reflection coefficient when the antenna was mounted onto the body compared to free-space. This reduction in variation is useful as it allows better characterisation of the antenna off the body. This can be beneficial when measuring moving body area network channels, as the antenna effects remain more stable, allowing for characterisation of the variations in the channel, while being aware of the antenna response, instead of measuring a combination of the varying channel and antenna. The free-space characteristics of the modified antenna were analysed, finding a decrease in radiation into the body of up to 4.7 dB. The modified antennas were also tested in a moving BAN channel measurement campaign, finding coherency time and fading depth of the UWB BAN channel. It was found that connections between the body and the wrist provided a significantly more variable channel, compared to connections around the torso.

Acknowledgment

The authors would like to thank COST2100 for funding a short term scientific mission, and Prof. Reiner Thomä, Dr. Rudolf Zetik and Ulrich Schwarz from Ilmenau University of Technology for their help with antenna measurement and channel sounder characterisation. The authors would also like to thank TREL (Toshiba Research Europe Limited) for their funding, support and allowing publication of this work. Funding was also attained from EPSRC (Engineering and physical research council) through the CASE (Cooperative Awards in Science and Engineering) scheme.

References

[1] R. Kohno, K. Hamaguchi, H.-B. Li, and K. Takizawa, "R&D and standardization of body area network (BAN) for medical healthcare," in *Ultra-Wideband, 2008. ICUWB 2008. IEEE International Conference on*, vol. 3, Sep. 2008, pp. 5–8.

[2] K. Yazdandoost and K. Sayrafian, "Channel model for body area network (BAN), ieee p802.15-08-0780-09-0006," *IEEE 802.15 Working Group Document*, April 2009.

[3] W. Hirt, "Ultra-wideband radio technology: overview and future research," *Computer Communications*, vol. 26, no. 1, pp. 46–52, February 2003.

[4] A. F. Molisch, D. Cassioli, C.-C. Chong, S. Emami, A. Fort, B. Kannan, J. Karedal, J. Kunisch, H. G. Schantz, K. Siwiak, and M. Z. Win, "IEEE 802.15.4a channel model - final report," *Tech. Rep., Document IEEE 802.1504-0062-02-004a*, 2005.

[5] A. Alomainy, Y. Hao, X. Hu, C. G. Parini, and P. S. Hall, "UWB on-body radio propagation and system modelling for wireless body-centric networks," in *Communications, IEE Proceedings-*, vol. 153, no. 1, Feb. 2006, pp. 107–114.

[6] M. Klemm and G. Troester, "EM energy absorption in the human body tissues due to UWB antenna," in *Progress In Electromagnetics Research, PIER 62*, 2006, pp. 261–280.

[7] A. Taparugssanagorn, C. Pomalaza-Raez, R. Tesi, M. Hamalainen, and J. Iinatti, “Effect of body motion and the type of antenna on the measured UWB channel characteristics in medical applications of wireless body area networks,” in *Ultra-Wideband, 2009. ICUWB 2009. IEEE International Conference on*, sept. 2009, pp. 332 –336.

[8] C. A. Balanis, *Antenna theory : analysis and design / Constantine A. Balanis*. J. Wiley, New York ; Brisbane :, 1982.

[9] SkyCross Inc, “SMT-3TO10M-A data sheet,” http://www.skycross.com/, 2009.

[10] M. Klemm and G. Troester, “Textile UWB antennas for wireless body area networks,” *IEEE Transactions on Antennas and Propagation*, vol. 54, no. 11, pp. 3192–3197, Nov. 2006.

[11] T. Zasowski, G. Meyer, F. Althaus, and A. Wittneben, “Propagation effects in UWB body area networks,” in *Ultra-Wideband, 2005. ICU 2005. 2005 IEEE International Conference on*, Sep. 2005, pp. 16–21.

[12] K. Watanabe, S. Hari, K. Ohno, and T. Ikegami, “Experiments on shadow effects of body and effective paths for UWB transmission in BAN,” in *Communications and Information Technologies, 2008. ISCIT 2008. International Symposium on*, oct. 2008, pp. 232 –237.

[13] T. Zasowski, G. Meyer, F. Althaus, and A. Wittneben, “UWB signal propagation at the human head,” vol. 54, no. 4, june 2006, pp. 1836 – 1845.

[14] J. Sachs, M. Kmec, P. Peyerl, P. Rauschenbach, R. Thom, and R. Zetik, “A novel ultra-wideband real-time MIMO channel sounder architecture,” in *XXVIII URSI G.A. proceedings*, New Delhi, India, Oct 2005.

[15] J. Jordan, P. Bishop, and B. Kiani, *Correlation-based measurement systems*, 1st ed. Ellis Horwood Ltd, 1989.

[16] A. Fort, J. Ryckaert, C. Desset, P. De Doncker, P. Wambacq, and L. Van Biesen, “Ultra-wideband channel model for communication around the human body,” *IEEE Journal on Selected Areas in Communications*, vol. 24, no. 4, pp. 927–933, Apr. 2006.

[17] A. Fort, C. Desset, P. De Doncker, P. Wambacq, and L. Van Biesen, “An ultra-wideband body area propagation channel model-from statistics to implementation,” *IEEE Transactions on Microwave Theory and Techniques*, vol. 54, no. 4, pp. 1820–1826, Jun. 2006.

[18] V. Roy and F. D. D. P. Stephane Oestges, Claude Horlin, “Propagation modeling for UWB body area networks: Power decay and multi-sensor correlations,” in *Spread Spectrum Techniques and Applications, 2008. ISSSTA ’08. IEEE 10th International Symposium on*, Aug. 2008, pp. 649–653.

[19] W. Thompson, K. Walker, R. Cepeda, M. Beach, and J. McGeehan, “Ultra wideband body area network channel measurement and analysis using textile antennas,” in *Antennas and Propagation for Body-Centric Wireless Communications, 2009 2nd IET Seminar on*, 20-20 2009, pp. 1 –5.

[20] R. DErrico and L. Ouvry, “Time-variant BAN channel characterization,” May 2009, cOST 2100 Meeting, Valencia, Spain.

[21] Qpar Angus Ltd, “WBHDP218SHG dual polar horn antenna datasheet,” http://www.q-par.com/, Sep 2007.

[22] Emerson & Cumings microwave products Inc, “ECCOSORB AN data sheet,” http://www.eccosorb.com/.

[23] R. Cepeda, W. Thompson, M. Beach, and J. McGeehan, “On the measurement and simulations of the frequency dependent path loss and MB-OFDM,” in *Ultra-Wideband, 2009. ICUWB 2009. IEEE International Conference on*, 9-11 2009, pp. 321 –325.

[24] A. Fort, C. Desset, J. Ryckaert, P. De Doncker, L. Van Biesen, and P. Wambacq, “Characterization of the ultra wideband body area propagation channel,” in *Ultra-Wideband, 2005. ICU 2005. 2005 IEEE International Conference on*, January 2005, pp. 5–8.

[25] Emerson & Cumings microwave products Inc, “ECCOSORB FGM-U data sheet,” http://www.eccosorb.com/.